Nonlocal fluxon dynamics in long Josephson junctions with Newtonian dissipative loss

2004 J. Phys.: Condens. Matter 16 S2715

(http://iopscience.iop.org/0953-8984/16/27/009)

INSTITUTE OF PHYSICS PUBLISHING JOURNAL OF PHYSICS: CONDENSED MATTER

J. Phys.: Condens. Matter **16** (2004) S2715–S2733 PII: S0953-8984(04)70868-1

Nonlocal fluxon dynamics in long Josephson junctions with Newtonian dissipative loss

H Rauh[1,3], **Y A Genenko**[1] **and C T Rieck**[2]

[1] Institut für Materialwissenschaft, Technische Universität Darmstadt, Petersenstrasse 23, D-64287 Darmstadt, Germany
[2] I. Institut für Theoretische Physik, Universität Hamburg, Jungiusstrasse 9, D-20355 Hamburg, Germany

E-mail: hera@tgm.tu-darmstadt.de

Received 23 October 2003
Published 25 June 2004
Online at stacks.iop.org/JPhysCM/16/S2715
doi:10.1088/0953-8984/16/27/009

Abstract

A model of a long Josephson junction described by a nonlocal governing fluxon equation, assuming Newtonian dissipation, is presented and studied analytically as well as numerically. From a ballistic trial solution for a steadily moving 2π phase difference kink based on an exact limiting form, observables such as the lower critical field for the appearance of Josephson vortices, the vortex magnetic field, the microscopic voltage across the tunnel layer, and the macroscopic voltage across the junction itself are derived and assessed for nonlocal effects. The current–voltage characteristic of the junction due to a regular array of Josephson vortices moving uniformly along it predominantly exhibits monostability when nonlocality is weak and dissipation high; however, a transition to bistability and associated formation of filaments of different current densities can occur when nonlocality is strong and dissipation low.

1. Introduction

A theoretical understanding of the electromagnetic properties of long Josephson junctions is important in at least two respects. Firstly, such junctions are characterized by soliton behaviour associated with the quantum of magnetic flux. Regarding superconducting electronics applications, the fact that the fluxon is a remarkably stable entity which can be stored, steered, manipulated and made to interact with devices other than those involving the respective junctions themselves suggests exploiting it as the basic bit in processing digital information [1]. Thus, microstrips of superconducting materials support, e.g., the ballistic transfer of a voltage pulse [2]; logic elements using long Josephson junctions offer the intriguing possibility to use their highly nonlinear current–voltage characteristic for switching at ultrafast speeds [3]. Similar features apply to Josephson gates based on multijunction interferometer instruments,

[3] Author to whom any correspondence should be addressed.

to junctions between thin superconducting films [4–6] and to sandwich structures, with the superconducting films deposited on insulated, flat superconducting shields [3]. Secondly, long Josephson junctions can play a model role in the physics of the solid state, since the capability of bulk or thin film high-temperature superconductors to carry loss-free currents is essentially limited by extended defects and by weak links between superconducting grains which often reveal Josephson junction-like traits [7]. As an established fact, dissipation in real inhomogeneous systems appears first due to the motion of weakly pinned Josephson vortices along some easy channels between the grains where the superconductor order parameter is reduced, rather than due to the motion of strongly pinned Abrikosov vortices inside the grains [8–10]. This constitutes a resistive mechanism similar to that in weak-link networks representative of granular superconducting sheets [11]. Whereas for conventional Josephson junctions with their low critical current density, and hence with a Josephson penetration depth by far surpassing the London penetration depth of the material bulk, a local electrodynamic description may be adequate, for weak links such as low-angle grain boundaries in high-quality specimens typified by a substantially increased critical current density, and hence by a Josephson penetration depth which could be much smaller than the London penetration depth of the material bulk, recourse to a nonlocal formulation must be made.

Previous studies of the electrodynamics of long Josephson junctions in the nonlocal regime, with the electric and magnetic fields due to Josephson vortex excitations described on the basis of the London and the Maxwell equations at hand, allowed for normal tunnel current dissipation by adopting a field-independent, ohmic quasiparticle conductivity, and obtained approximate solutions of the governing fluxon equation by considering vortex motion to be overdamped [12–18]. The transmission of tunnel junctions, however, is not in general linear, and hence the relation between the quasiparticle current density and the electric field does not always show an ohmic sign [19]. In this paper, therefore, we call upon an alternative, quadratic current–field dependence giving rise to Newtonian-type normal tunnel current dissipation [1]. Although fluxon dynamics involving this kind of dissipation is never overdamped and thus precludes simplifications analogous to those possible in the ohmic case, such a choice does have the distinct asset of yielding an exact, closed-form solution of the underlying fluxon equation, whatever the degree of dissipation, in the limit of locality, offering a convenient start for the set up of an approximate solution when nonlocality applies.

Proceeding from a geometric and electrodynamic characterization of the long Josephson junction addressed, in section 2 we briefly outline the derivation of the nonlocal fluxon equation for the space- and time-dependent phase difference of the superconductor order parameter across the tunnel layer of this junction, and provide relating expressions for observables associated with Josephson vortex excitations. Referring to steady-state motion of a 2π phase difference kink along the junction, with nonlocality present, in section 3 we establish a ballistic trial solution based on the corresponding, exactly solvable local case. In addition to rendering a complete analytic account, we also give useful limiting forms in the weakly and, respectively, strongly nonlocal regime. By employing the trial solution so defined, in section 4 we estimate electromagnetic properties due to single Josephson vortex excitations, viz the lower critical field, the vortex magnetic field, the pulse of the microscopic voltage across the tunnel layer, and the pulse of the macroscopic voltage across the junction itself. Moreover, we extend the present analysis to considering steady-state motion of a regular array of (noninteracting) Josephson vortices, allowing the current–voltage characteristic of the junction to be addressed as well. Apart from furnishing complete analytic accounts for each selected property, we again note limiting forms in the weakly and, respectively, strongly nonlocal regime. Finally, in section 5 we conclude by summarizing the results obtained and highlighting the implications of nonlocal effects. Details of mathematical evaluations can be found in appendices A, B and C.

2. Nonlocal fluxon equation

Let us consider an infinitely extended, one-dimensional Josephson junction made up of two identical superconductor banks occupying the half-spaces $-\infty < x \leqslant -d$ and $d \leqslant x < \infty$ with respect to a Cartesian system x, y, z and adjoining a nonmagnetic, normal metallic or lossy dielectric tunnel layer of thickness $2d$ filling the space $-d < x < d$. Typified as basic and characterized by the critical current density, j_c, the junction is thought to be driven by a distributed transport current of density $j_t < j_c$ flowing along the (positive) x-direction; a mode of operation realized, e.g., when both superconductor banks contain Abrikosov vortices in the critical state [20] such that a z-dependent magnetic field along the y-direction obtains.

Adopting the classical model of superconductivity, the electric and magnetic fields due to Josephson vortex excitations, $\boldsymbol{E}$ and $\boldsymbol{H}$—coexisting with the impressed Abrikosov vortices referred to above—in the superconductor regions are governed by the London equations [21]

$$\boldsymbol{E} = \mu_0 \lambda_L^2 \nabla \times \frac{\partial \boldsymbol{H}}{\partial t} \tag{1}$$

and

$$\boldsymbol{H} = -\lambda_L^2 \nabla \times (\nabla \times \boldsymbol{H}), \tag{2}$$

where μ_0 denotes the permeability of free space, λ_L is the London penetration depth, and t means time. In the tunnel layer region, these fields obey the Maxwell equation

$$\nabla \times \boldsymbol{H} = \varepsilon_r \varepsilon_0 \frac{\partial \boldsymbol{E}}{\partial t} + \boldsymbol{j}, \tag{3}$$

where ε_r indicates the relative permittivity of the tunnel layer, ε_0 is the permittivity of free space, and $\boldsymbol{j}$ stands for the density of the total tunnel current, reduced by the distributed transport current. In the entire space, furthermore, these fields satisfy the Maxwell equations

$$\nabla \times \boldsymbol{E} = -\mu_0 \frac{\partial \boldsymbol{H}}{\partial t} \tag{4}$$

and

$$\nabla \cdot \boldsymbol{E} = 0 \tag{5}$$

as well as

$$\nabla \cdot \boldsymbol{H} = 0. \tag{6}$$

The preceding equations are supplemented by the requirement of continuity of the components of $\boldsymbol{E}$ and $\boldsymbol{H}$ at $x = \pm d$, as well as by the condition that both fields and their spatial derivatives vanish when $x \to \pm\infty$ or, respectively, $z \to \pm\infty$.

With the geometry of the junction addressed, we assume that $\boldsymbol{E}$ has nonzero components E_x and E_z only, and hence that $\boldsymbol{H}$ has a nonzero component H_y only, depending, in general, on x, z and t. However, owing to the parallel plate structure assumed here, for a junction of half-thickness implied to be small compared to the characteristic electrodynamic lengths of the problem at hand, E_x and H_y do not vary with x inside the tunnel layer region, and the only nonvanishing component of the total current density is written as

$$j_x(z, t) = \Lambda |E_x| E_x + j_c \sin \varphi(z, t). \tag{7}$$

The first term herein specifies the density of the normal tunnel current adopting, for mathematical convenience, a field-dependent, nonohmic quasiparticle conductivity with a (positive) constant, Λ [1], and referring to experimental observations of this kind of dependence in junctions with some homogeneously doped superconductor banks [19]; the second term reflects the density of the Josephson supercurrent which, apart from the density of the critical

current, is determined by the phase difference of the superconductor order parameter across the tunnel layer, φ [3, 22]. From the definition of the corresponding microscopic voltage drop, $V = -2dE_x$, and the Josephson equation [23]

$$V(z,t) = -\left(\frac{\Phi_0}{2\pi}\right)\frac{\partial\varphi}{\partial t}, \tag{8}$$

where Φ_0 denotes the quantum of magnetic flux, it appears that the component E_x in equation (7), and hence the macroscopic voltage across the junction,

$$U(z,t) = -\int_{-\infty}^{\infty} E_x(x,z,t)\,\mathrm{d}x, \tag{9}$$

including losses in the superconductor banks as well, are related to $\partial\varphi/\partial t$. Likewise, equation (3) in conjunction with equation (7) shows that H_y is determined by $\partial\varphi/\partial z$. These field components—and allied electromagnetic quantities characteristic of Josephson vortex excitations—can therefore be calculated, once the dependence of φ on z and t is known.

In order to establish a governing equation for φ, we assume, according to the supposition stated before, that the half-thickness of the junction is much smaller than the London penetration depth; a condition certainly applying to most cases of practical significance. Furthermore, we introduce the normalized coordinates $\xi = x/\lambda_\mathrm{J}$, $\eta = y/\lambda_\mathrm{J}$, $\zeta = z/\lambda_\mathrm{J}$ and the normalized quantity $\delta = d/\lambda_\mathrm{J}$, with the Josephson penetration depth [3, 22]

$$\lambda_\mathrm{J} = \left(\frac{\Phi_0}{4\pi\mu_0\lambda_\mathrm{L} j_\mathrm{c}}\right)^{1/2}, \tag{10}$$

as well as the normalized time $\tau = \omega_\mathrm{J} t$, with the Josephson plasma frequency [3, 22]

$$\omega_\mathrm{J} = \left(\frac{4\pi d j_\mathrm{c}}{\varepsilon_\mathrm{r}\varepsilon_0\Phi_0}\right)^{1/2}. \tag{11}$$

Employing an approach detailed in previous work [12, 14–16], equation (3) under consideration of equations (1) and (2) as well as (4)–(8) then yields the nonlocal fluxon equation in the tunnel layer region,

$$\frac{\partial^2\varphi}{\partial\tau^2} + \frac{\alpha}{2}\left|\frac{\partial\varphi}{\partial\tau}\right|\frac{\partial\varphi}{\partial\tau} + \sin\varphi - \gamma = \frac{1}{\pi\varepsilon}\int_{-\infty}^{\infty}\mathrm{d}\zeta'\,K_0(|\zeta-\zeta'|/\varepsilon)\frac{\partial^2\varphi}{\partial\zeta'^2}, \tag{12}$$

with the dimensionless damping constant $\alpha = \Lambda\Phi_0/4\pi d\varepsilon_\mathrm{r}\varepsilon_0$, the normalized transport current density $\gamma = j_\mathrm{t}/j_\mathrm{c}$, the dimensionless nonlocality parameter $\varepsilon = \lambda_\mathrm{L}/\lambda_\mathrm{J}$, and the modified Bessel function of the second kind and order zero, K_0. We note that, owing to the ansatz for the density of the normal tunnel current in equation (7), the dissipative term associated with the first time-derivative in equation (12) is of Newtonian form. The dynamics of this equation thus shows that a distinction between oscillation and relaxation as in the case of a field-independent, ohmic quasiparticle conductivity, facilitating theoretical investigations through neglect of the second time-derivative in the overdamped regime, has no meaning here (cf [24, 25]). Hence, irrespective of the magnitude of α, all time-derivatives in equation (12) must be retained.

By means of a solution of equation (12), with appropriate initial and boundary conditions prescribed, the total electromagnetic energy associated with Josephson vortex excitations, per unit length of the junction in the η-direction, can be expressed as (cf [12–18])

$$W = \lim_{\gamma\to 0}\left\{\frac{\Phi_0}{2\pi}j_\mathrm{c}\lambda_\mathrm{J}\int_{-\infty}^{\infty}\mathrm{d}\zeta\,(1-\cos\varphi(\zeta,\tau)) + \frac{\Phi_0^2}{16\pi^3\mu_0\lambda_\mathrm{L}^2}\int_{-\infty}^{\infty}\mathrm{d}\zeta\left(\frac{\partial\varphi}{\partial\zeta}\right)\int_{-\infty}^{\infty}\mathrm{d}\zeta'\,K_0(|\zeta-\zeta'|/\varepsilon)\frac{\partial\varphi}{\partial\zeta'}\right\}. \tag{13}$$

The first term on the right-hand side of equation (13) represents the contribution of the Josephson supercurrent and the second term that of the self-induced magnetic field. Furthermore, the magnetic field component of Josephson vortex excitations, H_η, in the lower and the upper superconductor region, $-\infty < \xi \leqslant -\delta$ and $\delta \leqslant \xi < \infty$, respectively, can be put as (cf [14])

$$H_\eta(\xi, \zeta, \tau) = -\frac{\Phi_0}{4\pi^2\mu_0\lambda_L^2}\int_{-\infty}^{\infty} \mathrm{d}\zeta'\, K_0(((\xi \pm \delta)^2 + (\zeta - \zeta')^2)^{1/2}/\varepsilon)\frac{\partial\varphi}{\partial\zeta'}. \quad (14)$$

In the tunnel layer region, $-\delta < \xi < \delta$, itself, H_η is identical with the boundary values from equation (14), adopted on the surfaces of the superconductor banks. According to equation (8), the microscopic voltage across the tunnel layer follows from

$$V(\zeta, \tau) = -\left(\frac{\Phi_0}{2\pi}\right)\omega_J\frac{\partial\varphi}{\partial\tau}, \quad (15)$$

and the macroscopic voltage across the junction reads (cf [16])

$$U(\zeta, \tau) = -\left(\frac{\Phi_0}{4\pi\varepsilon}\right)\omega_J\int_{-\infty}^{\infty} \mathrm{d}\zeta' \exp(-|\zeta - \zeta'|/\varepsilon)\frac{\partial\varphi}{\partial\tau}. \quad (16)$$

3. Ballistic trial solution

Looking at steady-state vortex motion in the (positive) ζ-direction of the Josephson junction of infinite extent, we seek a ballistic solution of equation (12) represented by a single travelling 2π phase difference kink, i.e. by a topological soliton, depending on the coordinate $\chi = \zeta - u\tau$ alone, with slope $\mathrm{d}\varphi/\mathrm{d}\chi > 0$ throughout, assuming u is the kink velocity measured in units of the Swihart velocity $\upsilon = \lambda_J\omega_J$, the maximum velocity of electromagnetic wave propagation along the junction [26]. Such a solution obeys the integro-differential equation for φ in $-\infty < \chi < \infty$,

$$u^2\left(\frac{\mathrm{d}^2\varphi}{\mathrm{d}\chi^2} - \frac{\alpha}{2}\left|\frac{\mathrm{d}\varphi}{\mathrm{d}\chi}\right|\frac{\mathrm{d}\varphi}{\mathrm{d}\chi}\right) + \sin\varphi - \gamma = \frac{1}{\pi\varepsilon}\int_{-\infty}^{\infty} \mathrm{d}\chi'\, K_0(|\chi - \chi'|/\varepsilon)\frac{\mathrm{d}^2\varphi}{\mathrm{d}\chi'^2} \quad (17)$$

together with the boundary conditions

$$\lim_{\chi\to\infty}\varphi(\chi) - \lim_{\chi\to-\infty}\varphi(\chi) = 2\pi \quad (18)$$

and

$$\lim_{\chi\to\pm\infty}\frac{\mathrm{d}\varphi}{\mathrm{d}\chi} = 0; \quad (19)$$

it adopts equilibrium values determined by $\sin\varphi = \gamma$ and approached asymptotically as $\chi \to \pm\infty$.

In the local limit, defined by formally letting $j_c \to 0$ in equation (10), and hence $\varepsilon \to 0$, the respective coordinate becomes $\chi_0 = \zeta - u_0\tau$, and equation (17) reduces to the differential equation for φ_0 in $-\infty < \chi_0 < \infty$,

$$u_0^2\left(\frac{\mathrm{d}^2\varphi_0}{\mathrm{d}\chi_0^2} - \frac{\alpha}{2}\left|\frac{\mathrm{d}\varphi_0}{\mathrm{d}\chi_0}\right|\frac{\mathrm{d}\varphi_0}{\mathrm{d}\chi_0}\right) + \sin\varphi_0 - \gamma = \frac{\mathrm{d}^2\varphi_0}{\mathrm{d}\chi_0^2}, \quad (20)$$

the boundary conditions, equations (18) and (19), applying mutatis mutandis as well. Equation (20) has an appropriate exact, closed-form solution which, apart from an unimportant additive constant to χ_0, can be put as

$$\varphi_0(\chi_0) = 4\arctan(\exp(\chi_0/c_0)) + \arcsin\gamma, \quad (21)$$

with the dimensionless local kink half-width

$$c_0 = (\alpha/(\alpha(1-\gamma^2)^{1/2}+\gamma))^{1/2} \tag{22}$$

and the dimensionless local kink velocity

$$u_0 = (\gamma/(\alpha(1-\gamma^2)^{1/2}+\gamma))^{1/2} \tag{23}$$

(cf [1]). Instructive traits of this solution appear from the behaviour of the latter two quantities:

(i) the kink propagates with maximum velocity for zero damping or for the largest transport current, $u_0 \to 1$ if $\alpha \to 0$ when $0 < \gamma < 1$ or if $\gamma \to 1$ when $\alpha \geqslant 0$; conversely, it comes to a halt for zero transport current or for infinitely strong damping, $u_0 \to 0$ if $\gamma \to 0$ when $\alpha > 0$ or if $\alpha \to \infty$ when $0 \leqslant \gamma < 1$;

(ii) the travelling kink contracts to zero half-width for zero damping, $c_0 \to 0$ if $\alpha \to 0$ when $0 < \gamma < 1$, and assumes a damping-controlled half-width for the largest transport current, $c_0 \to \alpha^{1/2}$ if $\gamma \to 1$ when $\alpha \geqslant 0$;

(iii) the static kink expands to unit half-width for zero transport current, $c_0 \to 1$ if $\gamma \to 0$ when $\alpha > 0$, and adopts a transport current-controlled half-width for infinitely strong damping, $c_0 \to 1/(1-\gamma^2)^{1/4}$ if $\alpha \to \infty$ when $0 \leqslant \gamma < 1$.

Reverting to the problem of fluxon propagation when nonlocality is present, we invoke an approximate solution of equation (17) defined by

$$\varphi(\chi) = 4\arctan(\exp(\chi/c)) + \arcsin\gamma, \tag{24}$$

with the dimensionless nonlocal kink half-width c and the dimensionless nonlocal kink velocity u regarded as parameters to be defined such that the trial function, equation (24), which fulfills the boundary conditions, equations (18) and (19), gratifies equation (17) in a weighted averages sense and translates into the exact solution, equation (21), if $\varepsilon \to 0$. Multiplication of equation (17) by $\mathrm{d}\varphi/\mathrm{d}\chi$ and integration over χ links contributions from terms of this equation with even symmetry, yielding

$$\frac{\alpha u^2}{2}\int_{-\infty}^{\infty}\mathrm{d}\chi\left(\frac{\mathrm{d}\varphi}{\mathrm{d}\chi}\right)^3 - \gamma\int_{-\infty}^{\infty}\mathrm{d}\chi\left(\frac{\mathrm{d}\varphi}{\mathrm{d}\chi}\right) = 0; \tag{25}$$

an expression which reflects the balance between power dissipation associated with the flow of quasiparticles, and power supply effected by the driving transport current itself. When substituting equation (24) into (25), using equation (A.1) and observing (18), we obtain, with reference to equations (22) and (23), the conservation relation

$$u/c = u_0/c_0. \tag{26}$$

From equation (26) it appears that u can be calculated, once c is known. Likewise, multiplication of equation (17) by $\mathrm{d}^2\varphi/\mathrm{d}\chi^2$ and integration over χ singles out contributions from terms of this equation with odd symmetry, giving

$$u^2\int_{-\infty}^{\infty}\mathrm{d}\chi\left(\frac{\mathrm{d}^2\varphi}{\mathrm{d}\chi^2}\right)^2 + \int_{-\infty}^{\infty}\mathrm{d}\chi\left(\frac{\mathrm{d}^2\varphi}{\mathrm{d}\chi^2}\right)\sin\varphi(\chi) = \frac{1}{\pi\varepsilon}\int_{-\infty}^{\infty}\mathrm{d}\chi\left(\frac{\mathrm{d}^2\varphi}{\mathrm{d}\chi^2}\right)\int_{-\infty}^{\infty}\mathrm{d}\chi'\,K_0(|\chi-\chi'|/\varepsilon)\frac{\mathrm{d}^2\varphi}{\mathrm{d}\chi'^2}; \tag{27}$$

an expression constituted by the displacement current, the Josephson current and, respectively, the Josephson vortex magnetic field. When inserting equation (24) into (27) and exploiting equations (A.2), (A.3) as well as (A.11), we get, using equations (22), (23) and (26), the fixed-point relation

$$c = c_0 s^{1/2}(c/\varepsilon), \tag{28}$$

where

$$s(c/\varepsilon) = 6\pi(c/\varepsilon)^3 \sum_{n=1}^{\infty}(-1)^n n S'_{1,1}(n\pi c/\varepsilon), \tag{29}$$

in which $S'_{1,1}$ means the derivative with respect to the argument of the Lommel function of indices one. From equation (28), finally, c can be determined by iteration using, e.g., the local value $c = c_0$ for $\varepsilon = 0$ as a start.

The nonlocal regime is upward bounded by the fact that the critical current density of the Josephson junction must not exceed the depairing critical current density of the material bulk, $j_c < j_p$, confining ε to the (finite) range $0 \leqslant \varepsilon < \varepsilon_{max}$. Formally letting $j_c \to j_p$ in equation (10) yields the minimum value of the Josephson penetration depth,

$$\lambda_{J,min} = \left(\frac{\Phi_0}{4\pi\mu_0\lambda_L j_p}\right)^{1/2}, \tag{30}$$

and applying herein the estimate [21]

$$j_p \cong \frac{\Phi_0}{5\pi\mu_0\lambda_L^3}\kappa_{GL}, \tag{31}$$

with κ_{GL} denoting the Ginzburg–Landau parameter, renders the maximum value of the nonlocality parameter,

$$\varepsilon_{max} = \lambda_L/\lambda_{J,min} \cong \kappa_{GL}^{1/2}, \tag{32}$$

whence $\varepsilon_{max} \gg 1$ is seen to be typical of high-temperature superconductors.

Useful approximate representations of the nonlocal kink half-width and the nonlocal kink velocity obtain when considering ε to be either small or large. Thus, since in the weakly nonlocal regime, equation (29) with (A.13) yields

$$s(c/\varepsilon) = \{1 - \tfrac{7}{10}(\varepsilon/c)^2 + O((\varepsilon/c)^4)\}; \qquad 0 < \varepsilon \ll c, \tag{33}$$

employing equation (33) in (28) admits

$$c = c_0\{1 - \tfrac{7}{20}(\varepsilon/c_0)^2 + O((\varepsilon/c_0)^4)\}; \qquad 0 < \varepsilon \ll c_0, \tag{34}$$

and using equation (34) in (26) gives

$$u = u_0\{1 - \tfrac{7}{20}(\varepsilon/c_0)^2 + O((\varepsilon/c_0)^4)\}; \qquad 0 < \varepsilon \ll c_0. \tag{35}$$

Conversely, since in the strongly nonlocal regime, equation (29) with (A.15) yields

$$s(c/\varepsilon) \cong 4c/\pi\varepsilon; \qquad c \ll \varepsilon < \varepsilon_{max}, \tag{36}$$

employing equation (36) in (28) admits

$$c \cong (4/\pi\varepsilon)c_0^2; \qquad c_0 \ll \varepsilon < \varepsilon_{max}, \tag{37}$$

and using equation (37) in (26) gives

$$u \cong (4/\pi\varepsilon)c_0 u_0; \qquad c_0 \ll \varepsilon < \varepsilon_{max}. \tag{38}$$

Figures 1 and 2 illustrate the variation of the kink half-width and the kink velocity with the transport current density, calculated from equations (26) and (28), addressing various degrees of nonlocality and dissipation. This reveals that, while increasing nonlocality reduces the half-width of the kink, enlarged dissipation counteracts nonlocal effects, even causing a transition from a monotonic to a nonmonotonic dependence on the transport current density to occur. Whereas growing nonlocality also reduces the velocity of the kink, the interplay with dissipation here is such that a transition from a monotonic to a nonmonotonic dependence on the transport current density, subject to the degrees of nonlocality and dissipation, may or may not occur. We shall return to this point in a different context later.

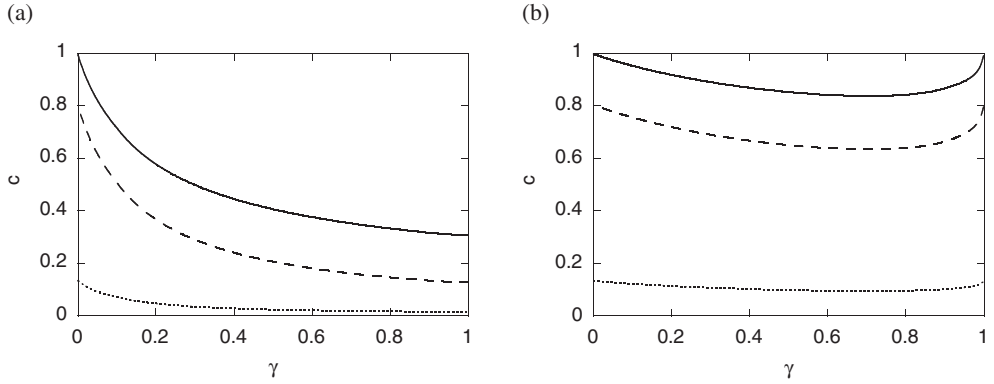

Figure 1. Kink half-width, c, as a function of the normalized transport current density, γ, for the nonlocality parameter $\varepsilon = 0.1$ (full curves), 1 (dashed curves), 10 (dotted curves), when the damping constant (a) $\alpha = 0.1$ and (b) $\alpha = 1$.

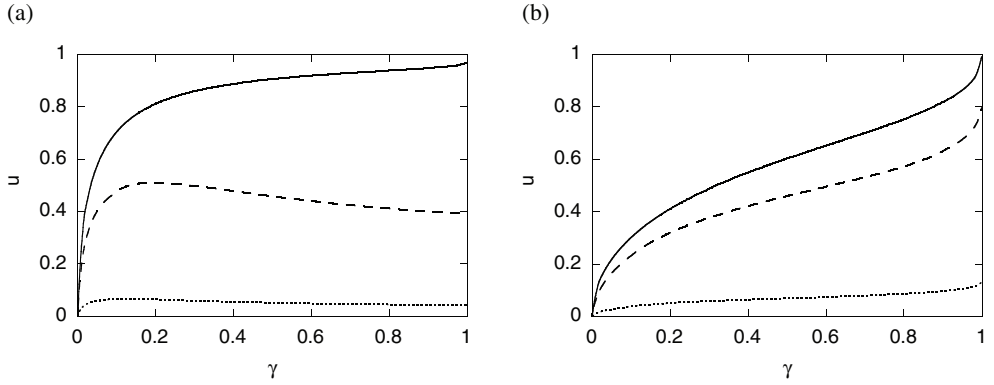

Figure 2. Kink velocity, u, as a function of the normalized transport current density, γ, for the nonlocality parameter $\varepsilon = 0.1$ (full curves), 1 (dashed curves), 10 (dotted curves), when the damping constant (a) $\alpha = 0.1$ and (b) $\alpha = 1$.

4. Electromagnetic properties

The ballistic trial solution, equation (24), describing steady-state propagation of a single phase difference kink allows convenient determinations of physical observables characteristic of the Josephson junction and its excitations. We consider the lower critical field, the vortex magnetic field, the microscopic and the macroscopic junction voltage as examples of such quantities.

4.1. Lower critical field

The lower critical field, i.e. the magnetic field at which a Josephson vortex appears first in the junction, ensues from the total electromagnetic energy associated with this kind of excitation, viz $H_{c1} = W/\Phi_0$ [21]. Following equation (13), it reads

$$H_{c1} = \lim_{\gamma\to 0}\left\{\frac{j_c\lambda_J}{2\pi}\int_{-\infty}^{\infty} d\chi\,(1-\cos\varphi(\chi)) + \frac{\Phi_0}{16\pi^3\mu_0\lambda_L^2}\int_{-\infty}^{\infty} d\chi\left(\frac{d\varphi}{d\chi}\right)\int_{-\infty}^{\infty} d\chi'\,K_0(|\chi-\chi'|/\varepsilon)\frac{d\varphi}{d\chi'}\right\}. \tag{39}$$

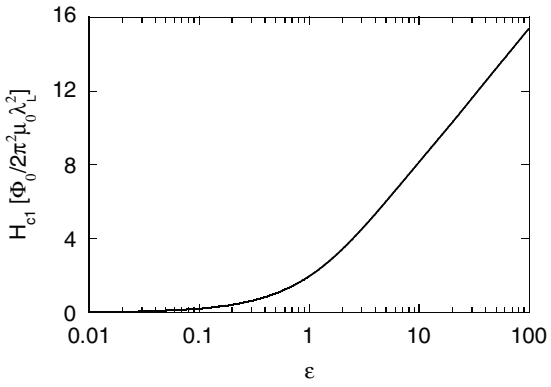

Figure 3. Lower critical field, H_{c1}, as a function of the nonlocality parameter, ε.

Employing the results of equations (B.1) and (B.7) in (39) and observing (10), we find

$$H_{c1} = \frac{\Phi_0}{2\pi^2\mu_0\lambda_L^2}\left\{\varepsilon c - 2\pi\sum_{n=1}^{\infty}(-1)^n n S_{0,0}(n\pi c/\varepsilon)\right\}, \tag{40}$$

where $S_{0,0}$ denotes the Lommel function of indices zero. The kink half-width c herein is governed by equation (28), with $c_0 = 1$ according to the limit $\gamma \to 0$ of equation (22), leaving a dependence on ε alone. Useful approximate representations obtain when considering ε to be either small or large. Thus, since in the weakly nonlocal regime, equation (40) with (B.9) yields

$$H_{c1} = \frac{\Phi_0}{2\pi^2\mu_0\lambda_L^2}\left\{\varepsilon c + \varepsilon/c - \frac{1}{6}(\varepsilon/c)^3 + \mathrm{O}((\varepsilon/c)^5)\right\}; \qquad 0 < \varepsilon \ll c, \tag{41}$$

employing equation (34) in (41) admits

$$H_{c1} = \frac{\Phi_0}{\pi^2\mu_0\lambda_L^2}\varepsilon\left\{1 - \frac{1}{12}\varepsilon^2 + \mathrm{O}(\varepsilon^4)\right\}; \qquad 0 < \varepsilon \ll c. \tag{42}$$

Conversely, since in the strongly nonlocal regime, equation (40) with (B.11) yields

$$H_{c1} \cong \frac{\Phi_0}{2\pi^2\mu_0\lambda_L^2}\left\{\varepsilon c + \frac{\pi}{2}\ln(\varepsilon/c)\right\}; \qquad c \ll \varepsilon < \varepsilon_{\max}, \tag{43}$$

exploiting equation (37) in (43) gives

$$H_{c1} \cong \frac{\Phi_0}{2\pi\mu_0\lambda_L^2}\ln\varepsilon; \qquad c \ll \varepsilon < \varepsilon_{\max}. \tag{44}$$

The variation of the lower critical field with the nonlocality parameter, calculated from equation (40), is displayed in figure 3. A linear rise for weak nonlocality followed by a transition towards a logarithmic increase for strong nonlocality can be clearly discerned. Suffice it to add that, as ε has an upper bound of $\varepsilon_{\max}$, Josephson vortices will only exist below the maximum critical field

$$H_{c1,\max} \cong \frac{\Phi_0}{2\pi\mu_0\lambda_L^2}\ln\varepsilon_{\max}; \qquad c \ll \varepsilon_{\max}, \tag{45}$$

which, from equation (32), also admits

$$H_{c1,\max} \cong \frac{\Phi_0}{4\pi\mu_0\lambda_L^2}\ln\kappa_{GL}; \qquad c \ll \kappa_{GL}. \tag{46}$$

This result agrees with the lower critical field for the first entry of Abrikosov vortices into the superconductor bulk [21].

4.2. Vortex magnetic field

Attending to equation (14), the magnetic field component of a Josephson vortex excitation, H_η, in the lower and the upper superconductor region, $-\infty < \xi \leqslant -\delta$ and $\delta \leqslant \xi < \infty$, respectively, moving along the junction with constant velocity u takes the form

$$H_\eta(\xi, \chi) = -\frac{\Phi_0}{4\pi^2\mu_0\lambda_L^2}\int_{-\infty}^{\infty} \mathrm{d}\chi'\, K_0(((\xi \pm \delta)^2 + (\chi - \chi')^2)^{1/2}/\varepsilon)\frac{\mathrm{d}\varphi}{\mathrm{d}\chi'}, \quad (47)$$

which, from equation (18), is seen to support a total of one quantum of magnetic flux. In the tunnel layer region, $-\delta < \xi < \delta$, itself, H_η is identical with the boundary values from equation (47), adopted on the surfaces of the superconductor banks. Useful approximate representations obtain when considering ε to be either small or large. Thus, in the weakly nonlocal regime, expanding the derivative in the integrand of equation (47) into a Taylor series and interchanging the order of summation and integration yields

$$H_\eta(\xi, \chi) = -\frac{\Phi_0}{4\pi^2\mu_0\lambda_L^2}\sum_{n=0}^{\infty}\frac{1}{(2n)!}\frac{\mathrm{d}^{2n}}{\mathrm{d}\chi^{2n}}\left(\frac{\mathrm{d}\varphi}{\mathrm{d}\chi}\right)\int_{-\infty}^{\infty}\mathrm{d}\chi'\, K_0(((\xi \pm \delta)^2 + \chi'^2)^{1/2}/\varepsilon)\chi'^{2n};$$
$$0 < \varepsilon \ll c. \quad (48)$$

Performing the integration in equation (48) with the help of [27, 28] gives

$$H_\eta(\xi, \chi) = -\frac{1}{(2\pi)^{1/2}}\left(\frac{\Phi_0}{\pi c\mu_0\lambda_L^2}\right)\sum_{n=0}^{\infty}\frac{2n+1}{(2n)!!}\varepsilon^{n+1/2}|\xi \pm \delta|^{n+1/2}$$
$$\times K_{n+1/2}(|\xi \pm \delta|/\varepsilon)\frac{\mathrm{d}^{2n}}{\mathrm{d}\chi^{2n}}\operatorname{sech}(\chi/c); \qquad 0 < \varepsilon \ll c, \quad (49)$$

where $K_{n+1/2}$ denotes modified spherical Bessel functions of the third kind and order $n + 1/2$, whence

$$H_\eta(\xi, \chi) = -\frac{\Phi_0}{2\pi\mu_0\lambda_L^2}(\varepsilon/c)\exp(-|\xi \pm \delta|/\varepsilon)\operatorname{sech}(\chi/c)\left\{1 - \frac{3}{2}(\varepsilon/c^2)(|\xi \pm \delta| + \varepsilon)\right.$$
$$\left.\times\,(2\operatorname{sech}^2(\chi/c) - 1) + \mathrm{O}((\varepsilon/c^2)^2)\right\}; \qquad 0 < \varepsilon \ll c, \quad (50)$$

c and u herein being determined by the respective equations (34) and (35). In the strongly nonlocal regime, on the other hand, approximating equation (47) by

$$H_\eta(\xi, \chi) \cong -\frac{\Phi_0}{4\pi^2\mu_0\lambda_L^2}K_0(((\xi \pm \delta)^2 + \chi^2)^{1/2}/\varepsilon)\int_{-\infty}^{\infty}\mathrm{d}\chi'\left(\frac{\mathrm{d}\varphi}{\mathrm{d}\chi'}\right); \qquad c \ll \varepsilon < \varepsilon_{\max} \quad (51)$$

and observing equation (18) yields

$$H_\eta(\xi, \chi) \cong -\frac{\Phi_0}{2\pi\mu_0\lambda_L^2}K_0(((\xi \pm \delta)^2 + \chi^2)^{1/2}/\varepsilon); \qquad c \ll \varepsilon < \varepsilon_{\max}, \quad (52)$$

c and u herein being determined by the respective equations (37) and (38); a result which agrees with the magnetic field component of an Abrikosov vortex excitation in the superconductor bulk [21], understanding here the absence of a normal vortex core. Contour lines of the magnetic field of a Josephson vortex excitation, derived from equation (47) for moderate dissipation, a medium transport current density and two different degrees of nonlocality, are displayed in figure 4, demonstrating a true Josephson character with their pronounced lenticular shapes, when nonlocality is weak, and confirming the Abrikosov-like character with their almost circular shapes, when nonlocality is strong.

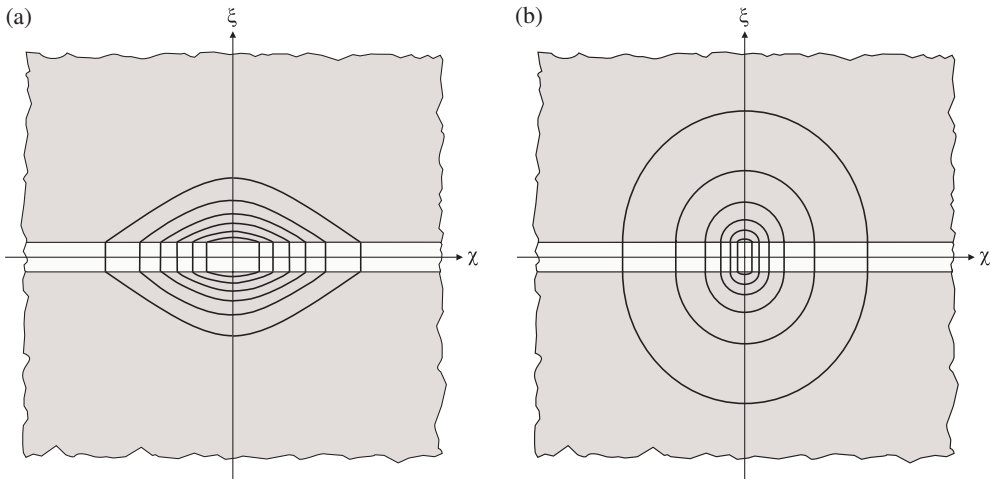

Figure 4. Contour lines of the magnetic field of a single moving Josephson vortex, H_η, for the damping constant $\alpha = 0.5$ and the normalized transport current density $\gamma = 0.5$, when the nonlocality parameter (a) $\varepsilon = 0.1$ and (b) $\varepsilon = 10$. The superconductor banks (dark shading), the tunnel layer (light shading) and the moving Cartesian system ξ, η, χ are marked.

4.3. Microscopic voltage

Following equation (15), the microscopic voltage across the tunnel layer, caused by a single Josephson vortex moving along the junction with constant velocity u according to equation (26) with (22), (23) and (28), takes the form

$$V(\chi) = \left(\frac{\Phi_0}{2\pi}\right) u\omega_J \frac{\mathrm{d}\varphi}{\mathrm{d}\chi}. \tag{53}$$

By exploiting equation (26) with (22) and (23), equation (53) yields

$$V(\chi) = \left(\frac{\Phi_0}{\pi}\right)\left(\frac{\gamma}{\alpha}\right)^{1/2} \omega_J \operatorname{sech}(\chi/c), \tag{54}$$

c herein being given by equation (28). Figure 5 shows the variation of the microscopic voltage with the coordinate along the junction, calculated from equation (54) for a medium transport current density, addressing various degrees of nonlocality and dissipation. It is obvious that, while increasing nonlocality tends to contract the microscopic voltage pulse, augmenting dissipation tends to spread this pulse and to reduce its height.

4.4. Macroscopic voltage

Attending to equation (16), the macroscopic voltage across the junction, caused by a single Josephson vortex moving along the junction with constant velocity u according to equation (26) with (22), (23) and (28), takes the form

$$U(\chi) = \left(\frac{\Phi_0}{4\pi\varepsilon}\right) u\omega_J \int_{-\infty}^{\infty} \mathrm{d}\chi' \exp(-|\chi - \chi'|/\varepsilon) \frac{\mathrm{d}\varphi}{\mathrm{d}\chi'}. \tag{55}$$

Useful approximate representations obtain when considering ε to be either small or large. Thus, in the weakly nonlocal regime, expanding the derivative in the integrand of equation (55) into

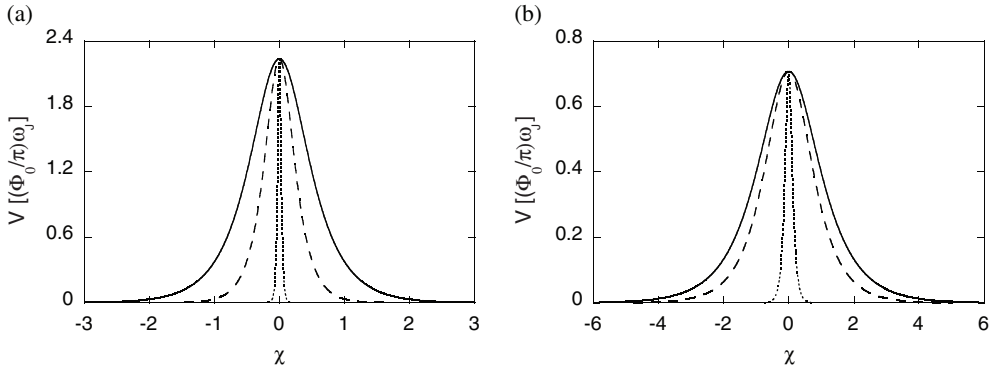

Figure 5. Microscopic voltage across the tunnel layer due to a single moving Josephson vortex, V, as a function of the normalized coordinate, χ, for the normalized transport current density $\gamma = 0.5$ and the nonlocality parameter $\varepsilon = 0.1$ (full curves), 1 (dashed curves), 10 (dotted curves), when the damping constant (a) $\alpha = 0.1$ and (b) $\alpha = 1$.

a Taylor series and interchanging the order of summation and integration yields

$$U(\chi) = \left(\frac{\Phi_0}{4\pi\varepsilon}\right) u\omega_{\mathrm{J}} \sum_{n=0}^{\infty} \frac{1}{(2n)!} \frac{\mathrm{d}^{2n}}{\mathrm{d}\chi^{2n}} \left(\frac{\mathrm{d}\varphi}{\mathrm{d}\chi}\right) \int_{-\infty}^{\infty} \mathrm{d}\chi' \exp(-|\chi'|/\varepsilon)\chi'^{2n}; \qquad 0 < \varepsilon \ll c. \tag{56}$$

Performing the integration in equation (56) with the help of [28] and exploiting equation (26) with (22) and (23) yields

$$U(\chi) = \left(\frac{\Phi_0}{\pi}\right)\left(\frac{\gamma}{\alpha}\right)^{1/2} \omega_{\mathrm{J}} \sum_{n=0}^{\infty} \varepsilon^{2n} \frac{\mathrm{d}^{2n}}{\mathrm{d}\chi^{2n}} \operatorname{sech}(\chi/c); \qquad 0 < \varepsilon \ll c, \tag{57}$$

that is

$$U(\chi) = \left(\frac{\Phi_0}{\pi}\right)\left(\frac{\gamma}{\alpha}\right)^{1/2} \omega_{\mathrm{J}} \operatorname{sech}(\chi/c)\{1 - (\varepsilon/c)^2(2\operatorname{sech}^2(\chi/c) - 1) + \mathrm{O}((\varepsilon/c)^4)\}; \quad 0 < \varepsilon \ll c, \tag{58}$$

c and u herein being given by equations (34) and (35), respectively; a result which, in the limit $\varepsilon \to 0$, reverts to the local form of equation (54). By contrast, in the strongly nonlocal regime, approximating equation (55) by

$$U(\chi) \cong \left(\frac{\Phi_0}{4\pi\varepsilon}\right) u\omega_{\mathrm{J}} \exp(-|\chi|/\varepsilon) \int_{-\infty}^{\infty} \mathrm{d}\chi' \left(\frac{\mathrm{d}\varphi}{\mathrm{d}\chi'}\right); \qquad c \ll \varepsilon < \varepsilon_{\max} \tag{59}$$

and observing equation (18) yields

$$U(\chi) \cong \left(\frac{\Phi_0}{2\varepsilon}\right) u\omega_{\mathrm{J}} \exp(-|\chi|/\varepsilon); \qquad c \ll \varepsilon < \varepsilon_{\max}, \tag{60}$$

c and u herein being determined by equations (37) and (38), respectively. Figure 6 illustrates the variation of the macroscopic voltage with the coordinate along the junction calculated from equation (55), again for a medium transport current density, addressing various degrees of nonlocality and dissipation. Evidently, increasing nonlocality tends to broaden the macroscopic voltage pulse, unlike the microscopic voltage pulse dealt with before, whereas augmenting dissipation tends to spread the macroscopic voltage pulse and to reduce its height, like the microscopic voltage pulse considered before.

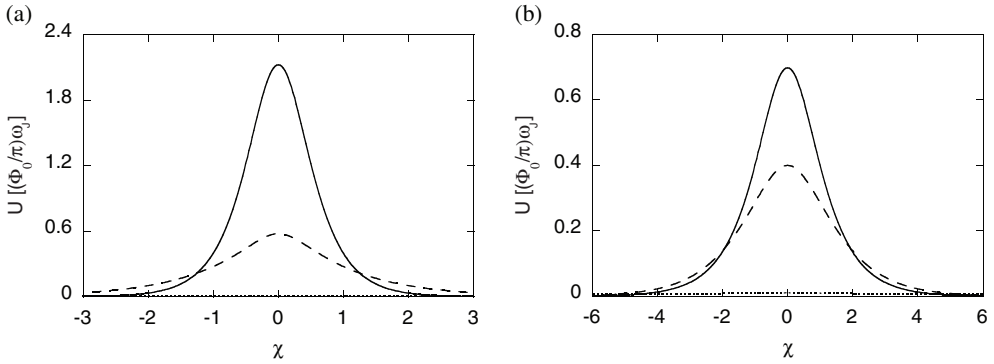

Figure 6. Macroscopic voltage across the junction due to a single moving Josephson vortex, U, as a function of the normalized coordinate, χ, for the normalized transport current density $\gamma = 0.5$ and the nonlocality parameter $\varepsilon = 0.1$ (full curves), 1 (dashed curves), 10 (dotted curves), when the damping constant (a) $\alpha = 0.1$ and (b) $\alpha = 1$.

The preceding analysis can be straightforwardly extended to a regular array of Josephson vortices, having normalized nearest-neighbour spacing $a \gg 2c$ such that interactions between individual vortices are negligible, and moving uniformly with velocity u according to equation (26) with (22), (23) and (28). The average macroscopic voltage across the junction caused by this array—a directly measurable quantity—is defined by

$$\langle U \rangle = \sum_{m=-\infty}^{\infty} \frac{1}{a} \int_0^a \mathrm{d}\chi \, U(\chi - ma). \tag{61}$$

Substituting equation (55) into (61) gives

$$\langle U \rangle = \left(\frac{\Phi_0}{4\pi a \varepsilon} \right) u \omega_J \int_0^a \mathrm{d}\chi \sum_{m=-\infty}^{\infty} \int_{-\infty}^{\infty} \mathrm{d}\chi' \exp(-|\chi - ma - \chi'|/\varepsilon) \frac{\mathrm{d}\varphi}{\mathrm{d}\chi'}. \tag{62}$$

Employing the result, equation (C.6), in (62) yields the simple form

$$\langle U \rangle = \left(\frac{\Phi_0}{a} \right) u \omega_J; \tag{63}$$

a proportionality to the velocity of the kink which, from its derivation, holds in the entire nonlocal regime. Useful approximate representations obtain when considering ε to be either small or large. Thus, in the weakly nonlocal regime, substituting equation (35) into (63) yields

$$\langle U \rangle = \left(\frac{\Phi_0}{a} \right) u_0 \omega_J \left\{ 1 - \frac{7}{20} (\varepsilon/c_0)^2 + \mathrm{O}((\varepsilon/c_0)^4) \right\}; \qquad 0 < \varepsilon \ll c_0. \tag{64}$$

Conversely, in the strongly nonlocal regime, substituting equation (38) into (63) gives

$$\langle U \rangle \cong \left(\frac{4\Phi_0}{\pi a \varepsilon} \right) c_0 u_0 \omega_J; \qquad c_0 \ll \varepsilon < \varepsilon_{\max}. \tag{65}$$

Figure 7 shows the average macroscopic voltage as a function of the normalized transport current density, i.e. the current–voltage characteristic of the Josephson junction at hand, based on numerical evaluations of equation (63) in conjunction with (26) and (28), addressing various degrees of dissipation and nonlocality. A general trait due to the interplay between the normal tunnel current and the Josephson supercurrent is the decrease of the initial voltage change with increasing dissipative loss. However, whereas the voltage itself rises monotonically with the

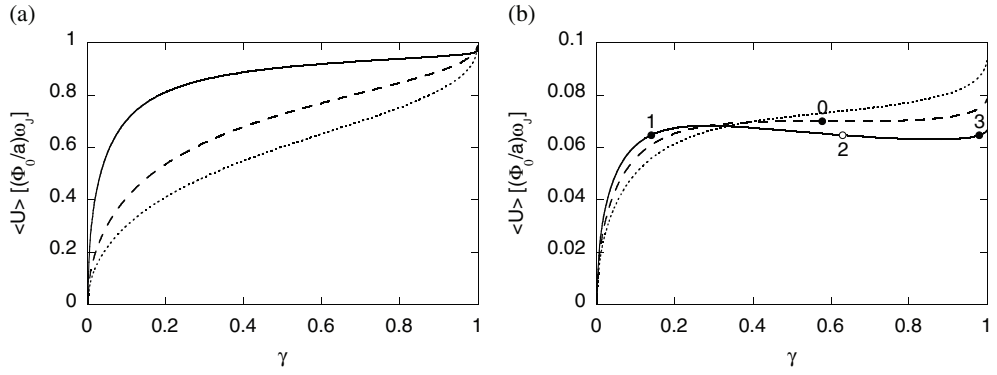

Figure 7. Average macroscopic voltage across the junction due to a moving array of Josephson vortices, $\langle U \rangle$, as a function of the normalized transport current density, γ, for (a) the damping constant $\alpha = 0.1$ (full curve), 0.5 (dashed curve), 1 (dotted curve), when the nonlocality parameter $\varepsilon = 0.1$, and for (b) the damping constant $\alpha = 0.25$ (full curve), 0.35 (dashed curve), 0.5 (dotted curve), when the nonlocality parameter $\varepsilon = 10$.

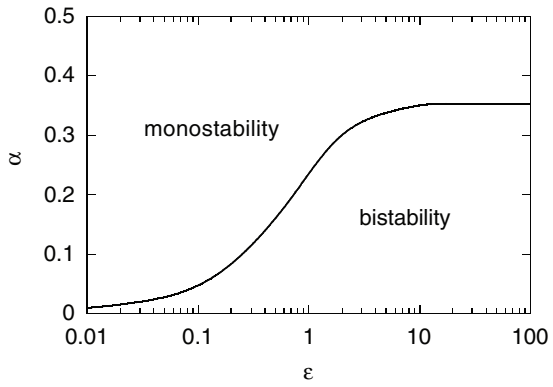

Figure 8. Stability chart for the current–voltage characteristic of the Josephson junction. The regions of monostability and bistability are separated by the critical damping constant, $\alpha = \alpha_c$, subject to the nonlocality parameter, ε.

transport current density for the values of the damping constant used, when nonlocality is weak (cf figure 7(a)), a nonmonotonic dependence subject to the values of the damping constant can occur, when nonlocality is strong; the average macroscopic voltage then falls across that range of the transport current density, where a negative differential resistance appears (cf figure 7(b)).

In experiments with a fixed voltage applied, rather than a uniform current impressed, characteristics of the latter type are always associated with instabilities. Thus, while for all points of the characteristic, monostability manifests itself at the highest dissipative loss, a branch point with zero slope, 0, emerges at the reduced, critical dissipative loss which, for a constant voltage maintained, splits into two stable points, 1 and 3, delineating the respective normalized current densities, γ_1 and γ_3, and encompassing an unstable point, 2, upon further reduction of the dissipative loss. This transition from monostability to bistability is not confined to the degree of nonlocality adopted here; it can occur throughout the nonlocal regime, as may easily be seen in figure 8. Recalling the phenomenon of current filamentation observed, e.g., in

junction devices using some homogeneously doped semiconductors under external conditions of the same kind [29], we therefore predict, when bistability exists, the formation of domains carrying currents of the normalized densities γ_1 and γ_3, aligned parallel to the direction of the transport current, for the Josephson junction too. The assumption of steady state requires the velocities, u_1 and u_3, together with the nearest-neighbour spacings, a_1 and a_3, distinguishing the array of Josephson vortices in the respective domains to adjust such that $u_1/a_1 = u_3/a_3$. The overall widths of these domains, w_1 and w_3, in turn are controlled by the average density of the current flowing along the filaments, $j_f = ((w_1\gamma_1 + w_3\gamma_3)/(w_1 + w_3))\, j_c$. Clearly, a more accurate analysis of current filamentation would have to take the current redistributions in the superconductor banks self-consistently into account.

5. Conclusions

Nonlocal fluxon dynamics in a long Josephson junction with Newtonian dissipative loss has been investigated both analytically and numerically. A ballistic trial solution of the underlying fluxon equation in the form of a steadily moving 2π phase difference kink based on the corresponding, exactly solvable local case has been set up and used to appraise nonlocal effects exhibited by various observable quantities. The results demonstrate that, whereas increasing nonlocality reduces the half-width of the kink and slows down its velocity of propagation, the critical field for the first appearance of Josephson vortices inside the junction tends to the limit at which Abrikosov vortices enter into the superconductor bulk. Accordingly, the contour lines of the magnetic field of Josephson vortex excitations show pronounced lenticular shapes when nonlocality is weak, but take on almost circular shapes when nonlocality is strong. Pulses of the microscopic voltage across the tunnel layer contract, while pulses of the macroscopic voltage across the junction itself broaden as a result of nonlocal effects. The current–voltage characteristic of the junction due to steady-state motion of a regular array of (noninteracting) Josephson vortices exhibits regions of monostability and bistability, depending on the extent of dissipation, at any degree of nonlocality, current filamentation being predicted, when bistability exists. Whereas in the region of bistability, and hence in the hysteretic mode, such junctions could mainly be employed for logic circuits [30], in the region of monostability, and hence in the nonhysteretic mode, they could predominantly be used for SQUIDs [31].

Appendix A. Evaluation of integrals related to the nonlocal fluxon equation

With the trial function, equation (24), the integrals [28]

$$\int_{-\infty}^{\infty} \mathrm{d}\chi \left(\frac{\mathrm{d}\varphi}{\mathrm{d}\chi}\right)^3 = \frac{8}{c^3}\int_{-\infty}^{\infty} \mathrm{d}\chi\, \mathrm{sech}^3(\chi/c) = \frac{4\pi}{c^2} \tag{A.1}$$

and

$$\int_{-\infty}^{\infty} \mathrm{d}\chi \left(\frac{\mathrm{d}^2\varphi}{\mathrm{d}\chi^2}\right)^2 = \frac{4}{c^4}\int_{-\infty}^{\infty} \mathrm{d}\chi\, \mathrm{sech}^2(\chi/c)\tanh^2(\chi/c) = \frac{8}{3c^3} \tag{A.2}$$

as well as

$$\begin{aligned}\int_{-\infty}^{\infty} \mathrm{d}\chi \left(\frac{\mathrm{d}^2\varphi}{\mathrm{d}\chi^2}\right)\sin\varphi(\chi) &= \frac{4}{c^2}(1-\gamma^2)^{1/2}\int_{-\infty}^{\infty} \mathrm{d}\chi\, \mathrm{sech}^2(\chi/c)\tanh^2(\chi/c) \\ &= \frac{8}{3c}(1-\gamma^2)^{1/2}\end{aligned} \tag{A.3}$$

hold; furthermore, from Parseval's relation and the convolution theorem [32], the representation

$$\int_{-\infty}^{\infty} \mathrm{d}\chi \left(\frac{\mathrm{d}^2\varphi}{\mathrm{d}\chi^2}\right) \int_{-\infty}^{\infty} \mathrm{d}\chi'\, K_0(|\chi - \chi'|/\varepsilon) \frac{\mathrm{d}^2\varphi}{\mathrm{d}\chi'^2} = \frac{4}{c^4} \int_{-\infty}^{\infty} \mathrm{d}\chi\, \mathrm{sech}(\chi/c) \tanh(\chi/c) \times \int_{-\infty}^{\infty} \mathrm{d}\chi'\, K_0(|\chi - \chi'|/\varepsilon)\, \mathrm{sech}(\chi'/c) \tanh(\chi'/c) = \frac{2}{\pi c^4} \int_{-\infty}^{\infty} \mathrm{d}\kappa\, f^*(\kappa) g(\kappa) f(\kappa); \qquad \varepsilon > 0, \quad c > 0 \tag{A.4}$$

applies, with Fourier transforms given by [28]

$$f(\kappa) = \int_{-\infty}^{\infty} \mathrm{d}\chi\, \mathrm{sech}(\chi/c) \tanh(\chi/c) \mathrm{e}^{\mathrm{i}\kappa\chi} = \mathrm{i}\pi c^2 \kappa\, \mathrm{sech}(\pi c\kappa/2) \tag{A.5}$$

and

$$g(\kappa) = \int_{-\infty}^{\infty} \mathrm{d}\chi\, K_0(|\chi|/\varepsilon) \mathrm{e}^{\mathrm{i}\kappa\chi} = \frac{\pi}{(\kappa^2 + 1/\varepsilon^2)^{1/2}}. \tag{A.6}$$

Using equations (A.5) and (A.6), the integral of the last equation (A.4) takes the form

$$\int_{-\infty}^{\infty} \mathrm{d}\kappa\, f^*(\kappa) g(\kappa) f(\kappa) = \frac{2\pi^3 c^4}{\varepsilon^2} \int_0^{\infty} \mathrm{d}\lambda \sinh^2\lambda\, \mathrm{sech}^2((\pi c/2\varepsilon)\sinh\lambda), \tag{A.7}$$

upon substituting $\varepsilon\kappa = \sinh\lambda$ and reducing the range of integration. The integral on the right-hand side of equation (A.7), which is readily amenable to efficient numerical evaluations, can be formally expressed in terms of a special function, as will be shown.

Expansion of the hyperbolic secant into a binomial series of exponentials [28] gives

$$\mathrm{sech}^2(\beta\sinh\lambda) = -4\sum_{n=1}^{\infty}(-1)^n n \exp(-2n\beta\sinh\lambda); \qquad \beta > 0, \quad \lambda > 0, \tag{A.8}$$

and Lommel's integrals [28] in conjunction with their recurrence relation [27] yield

$$S'_{1,1}(x) = -\int_0^{\infty} \mathrm{d}\lambda \sinh^2\lambda \exp(-x\sinh\lambda); \qquad x > 0, \tag{A.9}$$

i.e. an integral representation of the derivative of the Lommel function of indices one. Employing equations (A.8) and (A.9) imparts

$$\int_0^{\infty} \mathrm{d}\lambda \sinh^2\lambda\, \mathrm{sech}^2((\pi c/2\varepsilon)\sinh\lambda) = 4\sum_{n=1}^{\infty}(-1)^n n S'_{1,1}(n\pi c/\varepsilon). \tag{A.10}$$

Because of equations (A.7) and (A.10), equation (A.4) finally results in

$$\int_{-\infty}^{\infty} \mathrm{d}\chi \left(\frac{\mathrm{d}^2\varphi}{\mathrm{d}\chi^2}\right) \int_{-\infty}^{\infty} \mathrm{d}\chi'\, K_0(|\chi - \chi'|/\varepsilon) \frac{\mathrm{d}^2\varphi}{\mathrm{d}\chi'^2} = \left(\frac{4\pi}{\varepsilon}\right)^2 \sum_{n=1}^{\infty}(-1)^n n S'_{1,1}(n\pi c/\varepsilon). \tag{A.11}$$

Asymptotic expansion of the function $S_{1,1}$ [27, 28] admits

$$S'_{1,1}(x) \sim -2\left\{\frac{1}{x^3} - \frac{6}{x^5} + \mathrm{O}\left(\frac{1}{x^7}\right)\right\}; \qquad x \gg 1. \tag{A.12}$$

Using equation (A.12) in (A.11) and summing up the respective series of expansion coefficients [27] yields the approximate representation

$$\sum_{n=1}^{\infty}(-1)^n n S'_{1,1}(n\pi c/\varepsilon) = \frac{1}{6\pi}\left\{(\varepsilon/c)^3 - \frac{7}{10}(\varepsilon/c)^5 + \mathrm{O}((\varepsilon/c)^7)\right\}; \qquad 0 < \varepsilon \ll c. \tag{A.13}$$

Conversely, employing the form

$$\int_0^\infty \mathrm{d}\lambda \sinh^2\lambda \operatorname{sech}^2((\pi c/2\varepsilon)\sinh\lambda) \cong \frac{8}{3\pi^2}(\varepsilon/c)^2; \qquad c \ll \varepsilon < \varepsilon_{\max} \tag{A.14}$$

in equation (A.10) yields the approximate representation

$$\sum_{n=1}^{\infty}(-1)^n n S'_{1,1}(n\pi c/\varepsilon) \cong \frac{2}{3\pi^2}(\varepsilon/c)^2; \qquad c \ll \varepsilon < \varepsilon_{\max}. \tag{A.15}$$

Appendix B. Evaluation of integrals related to the lower critical field

With the trial function, equation (24), the limiting integral [28]

$$\lim_{\gamma\to 0}\int_{-\infty}^{\infty}\mathrm{d}\chi\,(1-\cos\varphi(\chi)) = 2\int_{-\infty}^{\infty}\mathrm{d}\chi\operatorname{sech}^2(\chi/c) = 4c \tag{B.1}$$

holds; furthermore, from Parseval's relation and the convolution theorem [32], the representation

$$\begin{aligned}\lim_{\gamma\to 0}\int_{-\infty}^{\infty}\mathrm{d}\chi\left(\frac{\mathrm{d}\varphi}{\mathrm{d}\chi}\right)\int_{-\infty}^{\infty}\mathrm{d}\chi' K_0(|\chi-\chi'|/\varepsilon)\frac{\mathrm{d}\varphi}{\mathrm{d}\chi'} \\ = \frac{4}{c^2}\int_{-\infty}^{\infty}\mathrm{d}\chi\operatorname{sech}(\chi/c)\int_{-\infty}^{\infty}\mathrm{d}\chi' K_0(|\chi-\chi'|/\varepsilon)\operatorname{sech}(\chi'/c) \\ = \frac{2}{\pi c^2}\int_{-\infty}^{\infty}\mathrm{d}\kappa\, h^*(\kappa)g(\kappa)h(\kappa); \qquad \varepsilon>0, \quad c>0\end{aligned} \tag{B.2}$$

applies, with Fourier transforms given by [28]

$$h(\kappa) = \int_{-\infty}^{\infty}\mathrm{d}\chi\operatorname{sech}(\chi/c)\mathrm{e}^{\mathrm{i}\kappa\chi} = \pi c\operatorname{sech}(\pi c\kappa/2) \tag{B.3}$$

and equation (A.6). Using equations (B.3) and (A.6), the integral of the last equation (B.2) takes the form

$$\int_{-\infty}^{\infty}\mathrm{d}\kappa\, h^*(\kappa)g(\kappa)h(\kappa) = 2\pi^3c^2\int_0^{\infty}\mathrm{d}\lambda\operatorname{sech}^2((\pi c/2\varepsilon)\sinh\lambda), \tag{B.4}$$

upon substituting $\varepsilon\kappa = \sinh\lambda$ and reducing the range of integration. The integral on the right-hand side of equation (B.4), which is readily amenable to efficient numerical evaluations, can be formally expressed in terms of a special function, as will be shown.

Employing the series expansion, equation (A.8), and the integral representation of the Lommel function of indices zero [28]

$$S_{0,0}(x) = \int_0^{\infty}\mathrm{d}\lambda\exp(-x\sinh\lambda); \qquad x>0 \tag{B.5}$$

imparts

$$\int_0^{\infty}\mathrm{d}\lambda\operatorname{sech}^2((\pi c/2\varepsilon)\sinh\lambda) = -4\sum_{n=1}^{\infty}(-1)^n n S_{0,0}(n\pi c/\varepsilon). \tag{B.6}$$

Because of equations (B.4) and (B.6), equation (B.2) finally results in

$$\lim_{\gamma\to 0}\int_{-\infty}^{\infty}\mathrm{d}\chi\left(\frac{\mathrm{d}\varphi}{\mathrm{d}\chi}\right)\int_{-\infty}^{\infty}\mathrm{d}\chi' K_0(|\chi-\chi'|/\varepsilon)\frac{\mathrm{d}\varphi}{\mathrm{d}\chi'} = -16\pi^2\sum_{n=1}^{\infty}(-1)^n n S_{0,0}(n\pi c/\varepsilon). \tag{B.7}$$

Asymptotic expansion of the function $S_{0,0}$ [27, 28] gives

$$S_{0,0}(x) \sim \left\{\frac{1}{x} - \frac{1}{x^3} + \mathrm{O}\left(\frac{1}{x^5}\right)\right\}; \qquad x \gg 1. \tag{B.8}$$

Using equation (B.8) in (B.7) and summing up the respective series of expansion coefficients [28] yields the approximate representation

$$\sum_{n=1}^{\infty}(-1)^n nS_{0,0}(n\pi c/\varepsilon) = -\frac{1}{2\pi}\left\{\varepsilon/c - \frac{1}{6}(\varepsilon/c)^3 + \mathrm{O}((\varepsilon/c)^5)\right\}; \qquad 0 < \varepsilon \ll c. \tag{B.9}$$

Conversely, employing the form

$$\int_0^{\infty} \mathrm{d}\lambda\, \mathrm{sech}^2((\pi c/2\varepsilon)\sinh\lambda) \mathrel{\tilde{=}} \ln(\varepsilon/c); \qquad c \ll \varepsilon < \varepsilon_{\max} \tag{B.10}$$

in equation (B.6) yields the approximate representation

$$\sum_{n=1}^{\infty}(-1)^n nS_{0,0}(n\pi c/\varepsilon) \mathrel{\tilde{=}} -\tfrac{1}{4}\ln(\varepsilon/c); \qquad c \ll \varepsilon < \varepsilon_{\max}. \tag{B.11}$$

Appendix C. Evaluation of integrals related to the macroscopic voltage

With the trial function, equation (24), and the convolution theorem [32], the representation

$$\int_{-\infty}^{\infty} \mathrm{d}\chi' \exp(-|\chi - \chi'|/\varepsilon)\frac{\mathrm{d}\varphi}{\mathrm{d}\chi'} = \frac{1}{\pi c}\int_{-\infty}^{\infty} \mathrm{d}\kappa\, e(\kappa)h(\kappa)\mathrm{e}^{-\mathrm{i}\kappa\chi}; \qquad \varepsilon > 0, \quad c > 0 \tag{C.1}$$

applies, with Fourier transforms given by [28]

$$e(\kappa) = \int_{-\infty}^{\infty} \mathrm{d}\chi \exp(-|\chi|/\varepsilon)\mathrm{e}^{\mathrm{i}\kappa\chi} = \frac{2/\varepsilon}{\kappa^2 + 1/\varepsilon^2} \tag{C.2}$$

and equation (B.3). Using equations (C.2) and (B.3), the last integral of equation (C.1) takes the form

$$\int_{-\infty}^{\infty} \mathrm{d}\kappa\, e(\kappa)h(\kappa)\mathrm{e}^{-\mathrm{i}\kappa\chi} = 2\pi c\int_{-\infty}^{\infty} \frac{\mathrm{d}\lambda}{\lambda^2 + 1}\,\mathrm{sech}(\pi c\lambda/2\varepsilon)\exp(-\mathrm{i}\lambda\chi/\varepsilon), \tag{C.3}$$

upon substituting $\varepsilon\kappa = \lambda$. With equations (C.1) and (C.3), the representation

$$\begin{aligned}\int_0^a \mathrm{d}\chi \sum_{m=-\infty}^{\infty}\int_{-\infty}^{\infty} \mathrm{d}\chi' \exp(-|\chi - ma - \chi'|/\varepsilon)\frac{\mathrm{d}\varphi}{\mathrm{d}\chi'} \\ = 2\int_{-\infty}^{\infty} \frac{\mathrm{d}\lambda}{\lambda^2 + 1}\,\mathrm{sech}(\pi c\lambda/2\varepsilon)\int_0^a \mathrm{d}\chi \exp(-\mathrm{i}\lambda\chi/\varepsilon)\sum_{m=-\infty}^{\infty}\exp(\mathrm{i}\lambda ma/\varepsilon)\end{aligned} \tag{C.4}$$

holds, upon reversing the order of summation and integration. Fourier series expansion of the Dirac delta function [32] admits

$$\sum_{m=-\infty}^{\infty}\exp(\mathrm{i}\lambda ma/\varepsilon) = (2\pi\varepsilon/a)\delta(\lambda), \tag{C.5}$$

so that equation (C.4) finally results in

$$\int_0^a \mathrm{d}\chi \sum_{m=-\infty}^{\infty}\int_{-\infty}^{\infty} \mathrm{d}\chi' \exp(-|\chi - ma - \chi'|/\varepsilon)\frac{\mathrm{d}\varphi}{\mathrm{d}\chi'} = 4\pi\varepsilon. \tag{C.6}$$

References

[1] Parmentier R D 1978 *Solitons in Action* ed K Lonngren and A Scott (New York: Academic) p 173
[2] Portis A M 1993 *Electrodynamics of High-Temperature Superconductors* (Singapore: World Scientific)
[3] Likharev K K 1991 *Dynamics of Josephson Junctions and Circuits* (Philadelphia: Gordon and Breach)
[4] Ivanchenko Y M and Soboleva T K 1990 *Phys. Lett.* A **147** 65
[5] Ivanchenko Y M and Soboleva T K 1990 *Sov. Phys.—JETP Lett.* **51** 114
[6] Ivanchenko Y M and Soboleva T K 1990 *Sov. Phys.—Solid State* **32** 1181
[7] Larbalestier D, Gurevich A, Feldman D M and Polyanskii A 2001 *Nature* **414** 368
[8] Diaz A, Mechin L, Bergius P and Evetts J E 1998 *Phys. Rev. Lett.* **80** 3855
[9] Diaz A, Mechin L, Bergius P and Evetts J E 1998 *Phys. Rev.* B **58** 2960
[10] Durrell J H, Hogg M J, Kahlmann F, Barber Z H, Blamire M G and Evetts J E 2003 *Phys. Rev. Lett.* **90** 247006
[11] Tinkham M and Lobb C B 1989 *Physical Properties of the New Superconductors* (New York: Academic)
[12] Aliev Y M, Silin V P and Uryupin S A 1992 *Superconductivity (Moscow)* **5** 228
[13] Aliev Y M, Silin V P and Uryupin S A 1993 *Sov. Phys.—JETP Lett.* **57** 193
[14] Aliev Y M and Silin V P 1993 *Sov. Phys.—JETP* **77** 142
[15] Gurevich A 1992 *Phys. Rev.* B **46** 3187
[16] Gurevich A 1993 *Phys. Rev.* B **48** 12857
[17] Gurevich A 1995 *Physica* C **243** 191
[18] Gurevich A 2002 *Phys. Rev.* B **65** 214531
[19] Wolf E L 1989 *Principles of Electron Tunneling Spectroscopy* (Oxford: University Press)
[20] Campbell A M and Evetts J E 1972 *Critical Currents in Superconductors* (London: Taylor and Francis)
[21] Tinkham M 1996 *Introduction to Superconductivity* (New York: McGraw-Hill)
[22] Barone A and Paternò G 1982 *Physics and Applications of the Josephson Effect* (New York: Wiley)
[23] Josephson B D 1962 *Phys. Lett.* **1** 251
[24] Andronov A A, Witt A A and Chaikin S E 1965 *Theorie der Schwingungen* part I (Berlin: Akademie)
[25] Andronov A A, Witt A A and Chaikin S E 1969 *Theorie der Schwingungen* part II (Berlin: Akademie)
[26] Swihart J C 1961 *J. Appl. Phys.* **32** 461
[27] Abramowitz M and Stegun I A 1972 *Handbook of Mathematical Functions* (New York: Dover)
[28] Gradshteyn I S and Ryzhik I M 1994 *Table of Integrals, Series and Products* (New York: Academic)
[29] Seeger K 2002 *Semiconductor Physics* (Berlin: Springer)
[30] Orlando T P and Delin K A 1991 *Foundations of Applied Superconductivity* (New York: Addison-Wesley)
[31] Gallop J C 1991 *SQUIDs, the Josephson Effects and Superconducting Electronics* (Bristol: Hilger)
[32] Arfken G B and Weber H J 1995 *Mathematical Methods for Physicists* (New York: Academic)